LOW RES

Thermal Structure and Metamorphic Evolution of Subducting Slabs

Simon M. Peacock

Department of Geological Sciences, Arizona State University, Tempe, Arizona

Variations in subduction-zone seismicity, seismic velocity, and arc magmatism reflect differences in the thermal structure and metamorphic reactions occurring in subducting oceanic lithosphere. Current kinematic and dynamical models of subduction zones predict cool slab-mantle interface temperatures less than one-half of the initial mantle temperature. Weak rocks along the slab-mantle interface likely limit the rate of shear heating; surface heat flux measurements and other observations suggest interface shear stresses are 0 - 40 MPa, consistent with this expectation. Thermal models of the NE Japan, Izu-Bonin, and Aleutian subduction zones predict slab-mantle interface temperatures of ~500 °C beneath the volcanic front. In such cool subduction zones, subducting oceanic crust transforms to eclogite at depths > 100 km and temperatures are too low to permit partial melting of subducted sediments or crust. In the Nankai subduction zone, where the incoming Philippine Sea Plate is unusually warm, predicted interface temperatures beneath sparse Holocene volcanoes are ~800 °C and eclogite transformation, slab dehydration reactions, and intermediate-depth seismicity occur at < 60 km depth. The geometry and vigor of mantle-wedge convection remains considerably uncertain; models incorporating strongly temperature-dependent mantle viscosity predict significantly higher slab-mantle interface temperatures.

INTRODUCTION

Subducting lithospheric plates are the cool, downwelling limbs of mantle convection and the negative buoyancy of subducting slabs (slab pull) drives plate tectonics [*Forsyth and Uyeda,* 1975]. Subduction zones are regions of intense earthquake activity, explosive volcanism, and complex mass transfer between the crust, mantle, hydrosphere, and atmosphere. In this contribution, I present subduction-zone thermal models that provide a framework for discussing the petrological and seismological processes that occur in subducting slabs (defined herein as the subducting sediments, oceanic crust, and oceanic mantle). Specific issues to be discussed include uncertainties regarding mantle-wedge convection, metamorphic reactions in the subducting plate, the origin of arc magmas, and subduction-zone earthquakes.

GENERAL OBSERVATIONS REGARDING SUBDUCTION ZONES

Subducting slabs are cool because oceanic lithosphere, the cold upper boundary layer of Earth's internal convection, descends into the mantle more rapidly than heat conduction warms the slab. The chilling effect of subduction is recorded by surface heat flux measurements < 0.03 W m^{-2} in subduction-zone forearcs (one-half of the average global surface heat flux). In well-studied subduction zones like Cascadia, forearc heat flux systematically decreases from the trench to the volcanic front [*Hyndman and Wang,* 1995].

Cold subducting slabs are well resolved as high-velocity regions in seismic tomography studies [e.g., *Zhao et al.,* 1994]. Low-temperature, high-pressure metamorphic rocks (blueschists, eclogites) provide an important record of the unusually cool temperatures at depth in subduction zones [e.g., *Carswell,* 1990; *Peacock,* 1992; *Hacker,* 1996].

Despite subducting slabs being cool compared to the surrounding mantle, almost all subduction zones are distinguished by active arc volcanism, which requires that rocks melt somewhere in the subduction zone system. Early thermal models of subduction zones assumed a priori that arc magmas were derived from direct melts of the subducting slab and these models incorporated high rates of shear heating along the slab-mantle interface in order to supply the required heat [e.g., *Oxburgh and Turcotte,* 1970; *Turcotte and Schubert,* 1973]. Over time, this view has evolved and most arc magmas are now thought to represent partial melts of the mantle wedge induced by infiltration of aqueous fluids derived from the subducting slab [e.g., *Gill,* 1981; *Hawkesworth et al.,* 1993]. Current thermal models of subduction zones call upon lower rates of shear heating and predict that slab melting only occurs in unusually warm subduction zones characterized by young incoming lithosphere and slow convergence [e.g., *Peacock et al.,* 1994]. The complex origin of arc magmas, however, remains an area of active research and debate.

THERMAL STRUCTURE OF SUBDUCTION ZONES

The thermal structure of subduction zones has been investigated using analytical [e.g., *Molnar and England,* 1990] and numerical techniques [e.g., *Toksöz et al.,* 1971; *Peacock,* 1990a; *Davies and Stevenson,* 1992; *Peacock et al.,* 1994; *Kincaid and Sacks,* 1997]. These studies have identified a number of important parameters that control the thermal structure of a subduction zone (Figure 1) including: (1) convergence rate, (2) thermal structure of the incoming lithosphere, which is primarily a function of lithospheric age but is also affected by hydrothermal cooling and the thickness of insulating sediments, (3) geometry of the subducting slab, (4) rate of shear heating (= shear stress x convergence rate), and (5) vigor and geometry of flow in the mantle wedge [see review by *Peacock,* 1996]. The first three parameters are relatively well constrained whereas the rate of shear heating and mantle wedge flow are considerably uncertain.

Calculated slab temperatures decrease with increasing convergence rate and increasing age of the incoming lithosphere. Most western Pacific subduction zones, such as the Kamchatka-Kurile-Honshu and Izu-Bonin-Mariana systems, are characterized by rapid convergence of old, cool lithosphere; subducted slabs in these subduction zones are relatively cool. In contrast, the young incoming lithosphere and modest convergence rates of subduction zones such as Nankai and Cascadia lead to relatively warm subducted slabs.

At shallow depths (<50 km), temperatures along the slab-mantle interface during the earliest stages of underthrusting are predicted to equal the average of the surface temperature (T_s) and the initial (pre-subduction) mantle temperature at the depth of interest (T_i) [*Molnar and England,* 1990]. Continued underthrusting removes heat from the upper plate and interface temperatures decrease to less than 0.5 (T_s + T_i). High rates of shear heating increase interface temperatures, but the low surface heat flux observed in forearcs requires that advective cooling, and not shear heating, controls the shallow thermal structure of subduction zones. In general, there is good agreement among the different thermal models presented in the literature and much of the apparent variation in published thermal structures results from different rates of shear heating. Recent studies, based on surface heat flow measurements and other data, suggest shear stresses in subduction zones are of order 10 MPa and range from 0 to 40 MPa (Table 1). Shear heating, while an important heat source, is not the primary control on temperatures in the subducting slab.

At depths greater than ~50 km, convection in the overlying mantle wedge strongly influences slab temperatures. Induced mantle-wedge convection warms the subducting slab and a cool boundary layer forms in the mantle wedge adjacent to the slab [e.g., *McKenzie,* 1969]. Mantle-wedge

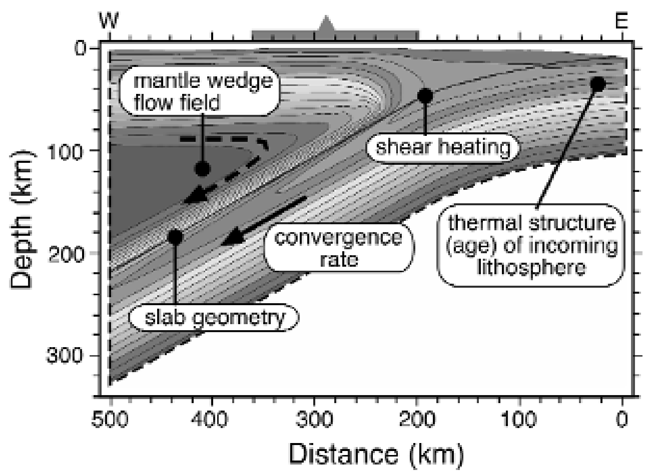

Figure 1. Important parameters which govern the thermal structure of a subduction zone.

convection increases slab-mantle interface temperatures by ~200-250 °C based on comparing *Molnar and England's* [1990] analytical expressions with the results of numerical models incorporating wedge convection (Figure 2). However, models with mantle-wedge convection still predict slab-mantle interface temperatures less than 0.5 (T_s + T_i) (Figure 2) [e.g., *Davies and Stevenson,* 1992; *Furukawa,* 1993; *Peacock et al.,* 1994; *Peacock,* 1996; *Kincaid and Sacks,* 1997].

THERMAL-PETROLOGIC MODELS OF COOL AND WARM SUBDUCTION ZONES

Recently, we constructed a set of two-dimensional, finite-element, thermal models of four subduction zones—NE Japan, Izu-Bonin, the Aleutians, and Nankai—in order to test thermal models against seismological and magmatic observations (Plate 1) [*Peacock and Wang,* 1999; *Peacock and Hyndman,* 1999; this study]. These models solve the steady-state heat transfer equation including terms for heat conduction, advection, and heat sources; in the case of Nankai we used a transient solution in order to account for the subduction of the young Shikoku basin. For each subduction zone, the geometry of the subducting slab is defined using seismic reflection and refraction studies at shallow levels and Wadati-Benioff zone seismicity at deeper levels. Our models include two heat sources: radiogenic heat production in the upper-plate crust and shear heating along the plate boundary from the trench to 70 km depth. We neglect heat transported by fluids and heat consumed (released) by endothermic (exothermic) reactions; both fluid advection and metamorphic reaction enthalpies are proportional to the amount of H_2O involved, which in subduction zones is very limited at depths > 10 km [*Peacock,* 1987; *Peacock,* 1990b]. The thermal structure of the incoming plate is fixed using an oceanic geotherm of appropriate age [*Stein and Stein,* 1992]. The arc-side boundary is defined by either a continental geotherm (surface heat flux = 0.065 W m^{-2}) or a 20 Ma oceanic geotherm in the case of the Izu-Bonin model. The surface temperature is fixed at 0 °C and the temperature at the base of the 95-km-thick subducting plate is fixed at 1450 °C [*Stein and Stein,* 1992]. Where material flows out of the model grid, no horizontal conductive heat flow is permitted.

These thermal models are "kinematic" in the sense that the slab geometry and convergence rate are model inputs, but we use a dynamical model for flow in the mantle wedge. In a pure "dynamical" model, the slab geometry and subduction

Table 1. Recent estimates of subduction zone shear stresses.

Subduction zone	Shear stress (MPa)	Reference
(1) Match of thermal models to surface heat flow		
Continental	14 - 27	*Tichelaar and Ruff* [1993]
Cascadia	~0	*Hyndman and Wang* 1995]
Nankai	~0	*Peacock and Wang* [1999]
NE Japan	10	*Peacock and Wang* [1999]
Kermadec	40 ± 17	*von Herzen et al.* [2001]
(2) Blueschists (high P – low T conditions)		
Franciscan	< 20 - 30	*Peacock* [1992]
Mariana	18 ± 8	*Peacock* [1996]
(3) Dynamical modeling of trench topography		
Oceanic	15 - 30	*Zhong and Gurnis* [1994]
(4) Upper plate stress field		
Cascadia	< 10	*Wang et al.* [1995]

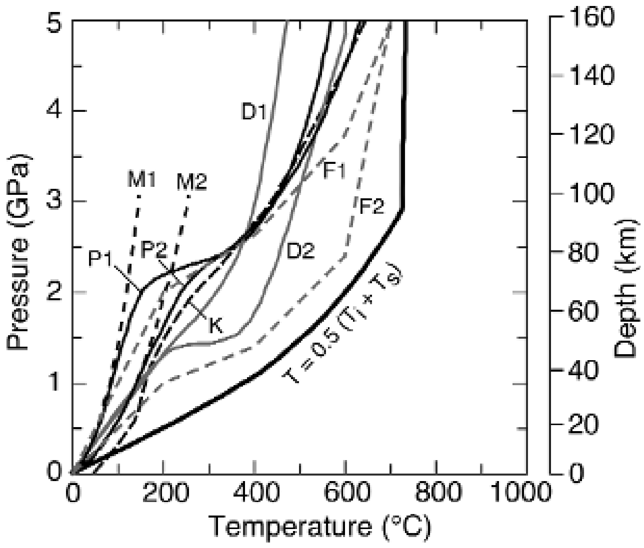

Figure 2. Predicted pressure-temperature conditions along the slab-mantle interface based on published kinematic and dynamical models. In each case predicted interface temperatures are less than one-half the sum of the surface temperature (T_s) and the initial, pre-subduction mantle temperature at depth (T_i). M1, M2; *Molnar and England's* [1990] analytical expressions for convergence rate, V = 100 and 30 mm yr^{-1}, respectively. D1, D2; *Davies and Stevenson's* [1992] numerical solutions for V = 72 mm yr^{-1} and 60° and 30°, respectively. F1, F2; *Furukawa's* [1993] numerical solutions for V = 100 mm yr^{-1} and a slab-wedge coupling depth of 100 and 40 km, respectively. P1, P2; *Peacock et al.'s* [1994] numerical solutions for V = 100 and 30 mm yr^{-1}, respectively. K, *Kincaid and Sack's* [1997] numerical solution for V = 100 mm yr^{-1}.

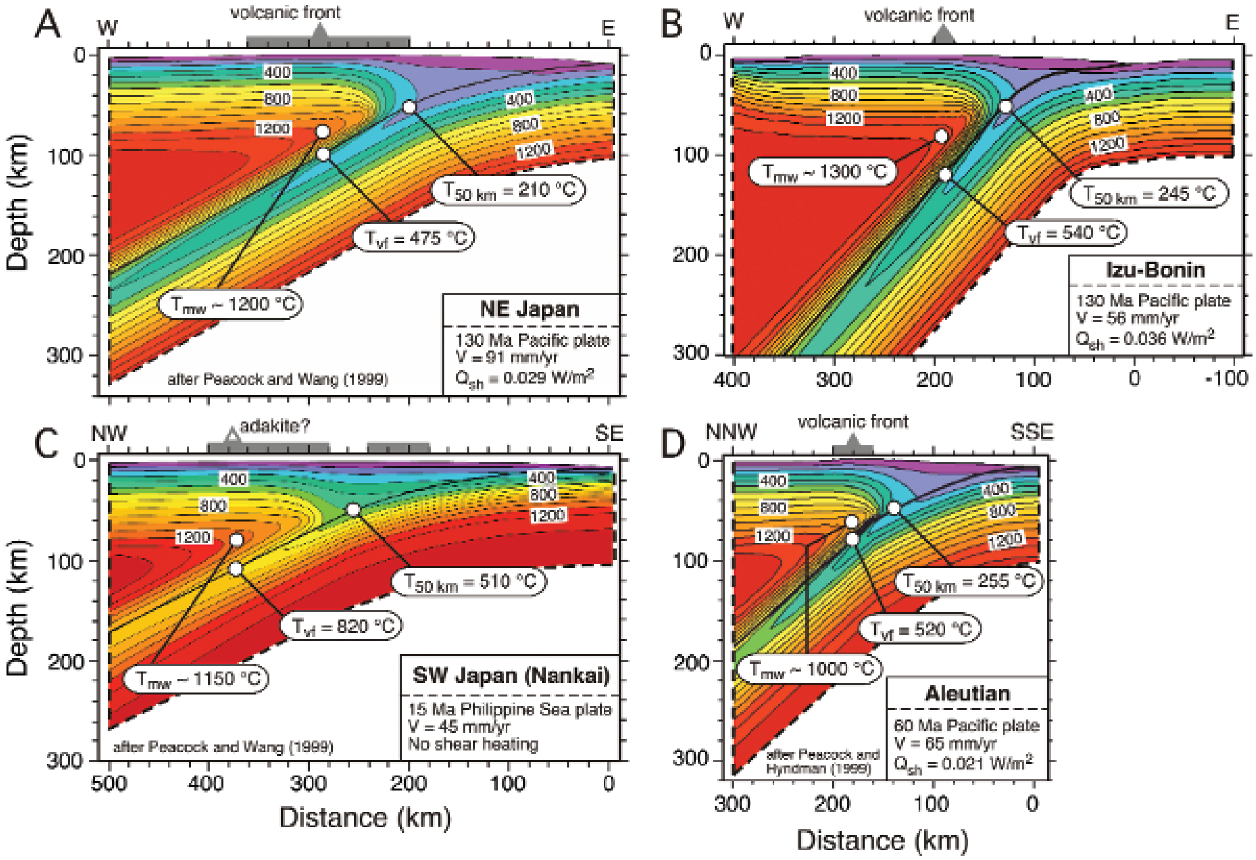

Plate 1. Calculated thermal structures for four different subduction zones. T_{50km}, Slab interface temperature at 50 km depth; T_{vf}, slab interface temperature directly beneath volcanic front; T_{mw}, maximum temperature in the mantle wedge directly beneath volcanic front. (A) NE Japan (Honshu) after *Peacock and Wang* [1999]. (B) SW Japan (Nankai) after *Peacock and Wang* [1999]. (C) Izu-Bonin (32 °N). (D) Aleutian Islands (Umnak) after *Peacock and Hyndman* [1999].

rate would be calculated based on internal and external forces. Velocities in the subducting slab are set equal to the orthogonal convergence rates determined using the NUVEL-1A plate motion model [*DeMets et al.,* 1994]. For the mantle wedge, we use a simple dynamical flow model of Newtonian viscous corner flow [*Batchelor,* 1967] driven by a no-slip boundary condition along the top of the subducting plate. Mantle-wedge flow occurs beneath a 50-km-thick rigid lithosphere and is truncated in the tip of the mantle wedge to satisfy surface heat flux data [*Peacock and Wang,* 1999].

Thermal models constructed for three cool subduction zones (NE Japan, Izu-Bonin, the Aleutians) and one relatively warm subduction zone (Nankai) are depicted in Plate 1. Calculated slab-mantle interface temperatures in the Nankai subduction zone are ~300 °C warmer than interface temperatures in the NE Japan, Izu-Bonin, and Aleutian subduction zones (Figure 3B). The high slab temperatures in Nankai reflect the hot incoming Philippine Sea Plate [*Wang et al.,* 1995; *Peacock and Wang,* 1999]. At 50 km depth, the calculated temperatures along the slab-mantle interface range from 210 to 255 °C for the three cool subduction zones as compared to 510 °C for the warmer Nankai subduction zone. Beneath the volcanic front the slab-mantle interface temperatures for the three cool subduction zones are similar, ranging from 475 to 540 °C. In contrast, beneath the sparse Holocene volcanoes in the Nankai subduction zone, the calculated slab-mantle interface temperature is 820 °C. Note the apparent paradox—warmer slab interface temperatures correlate with less productive volcanic arcs.

The key to resolving this paradox lies in the recognition that most arc magmas are generated not by slab melting, but by slab-derived aqueous fluids that infiltrate the hot core of the overlying mantle wedge [e.g., *Gill,* 1981]. In subduction zones with cool slabs, hydrous minerals are stable to depths > 100 km and H_2O is released beneath hot (> 1300 °C) mantle wedge capable of undergoing H_2O-flux melting. In subduction zones with warm slabs, hydrous minerals breakdown at depths < 100 km and H_2O infiltrates forearc mantle that is too cool to undergo partial melting. In the extreme, several subduction zones that lack volcanic arcs are characterized by very warm slabs as a result of flat slab geometry or subducting ridges.

Qualitatively, the calculated thermal structure of the mantle wedge is similar in all four subduction zones which is not surprising given the simple viscous corner-flow model. Heat transfer in the mantle wedge occurs primarily by advection such that isotherms in the mantle wedge closely follow material flow lines. Basaltic lavas present in many arcs require mantle temperatures greater than 1300 °C [e.g., *Tatsumi et al.,* 1983]. In all models the nose of the 1300 °C isotherm occurs at 80-95 km depth where the top of the underlying slab lies at 115-130 km depth. There is considerable variation among the four subduction zones in the depth to the subducting slab beneath the volcanic front. In the Izu-Bonin subduction zone, the depth to the slab beneath the volcanic front is 120 km as compared to only 80 km in the Aleutian subduction zone. This variation results in maximum mantle-wedge temperatures directly beneath the volcanic front ranging from ~1300 °C in the Izu-Bonin subduction zone to ~1000 °C in the Aleutian subduction zone. The uncertainties in mantle-wedge flow, discussed below, lead to considerable uncertainties in the calculated thermal structure of the mantle wedge beneath the volcanic arc. For example, higher wedge temperatures beneath the Aleutian arc would be generated by models assuming a temperature-dependent mantle viscosity and shallower viscous coupling depth.

CONVECTION IN THE MANTLE WEDGE

The geometry and vigor of mantle-wedge convection are poorly known and represent a major uncertainty in thermal models of subduction zones. Subducting slabs induce convection in the mantle wedge through mechanical and thermal coupling. Mechanical coupling (viscous traction) between the subducting slab and the base of the mantle wedge drives corner flow [*McKenzie,* 1969], a type of forced convection. The subducting slab also cools the base of the mantle wedge driving thermal convection (free convection); the cooler, denser base of the mantle wedge tends to sink together with the subducting slab [e.g., *Rabinowicz et al.,* 1980]. Thermal convection becomes increasingly important with decreasing viscosity. Hydration and partial melting may also be significant sources of buoyancy in parts of the mantle wedge.

In forced convection models, such as the models presented above, flow in the mantle wedge is driven solely by mechanical coupling to the subducting slab. For the case of constant wedge viscosity, the resulting corner-flow velocity field may be calculated analytically [*Batchelor,* 1967]. In constant viscosity corner flow, material flows into the mantle wedge along subhorizontal flow lines parallel to the base of the overriding lithosphere. Toward the wedge corner, the flow lines bend downward and become subparallel to the top of the subducting slab. In these models, mantle wedge flow is driven by the boundary conditions. The extent to which hot mantle flows into the forearc region depends on the thickness of the overlying "rigid" lithosphere [*Rowland and Davies,* 1999] and the depth at which slab-mantle coupling begins [*Furukawa,* 1993].

Forced convection mantle-wedge flow fields calculated using a *T*-dependent viscosity are qualitatively similar to constant viscosity flow fields because the velocity boundary condition along the top of the slab controls the overall flow structure [*Davies and Stevenson,* 1992]. Depending primarily on the model boundary conditions, temperature-dependent viscosity flow fields may closely resemble constant-viscosity corner flow fields [e.g., *Davies and Stevenson,* 1992] or may exhibit a significant upward component of motion beneath the overriding lithosphere [e.g., *Furukawa,* 1993]. The component of upward motion depends, in part, on the depth of the high-temperature isotherms on the arc-side boundary relative to the depth at which slab-wedge coupling begins [*Furukawa,* 1993; *Rowland and Davies,* 1999]. In *Furukawa's* [1993] models the upward component of wedge flow increases as the depth at which slab coupling begins decreases. Decreasing the depth of slab-wedge coupling from 100 km to 40 km increases slab surface temperatures by as much as 300 °C at 65 km depth (Figure 2) [*Furukawa,* 1993]. At present, the depth at which full slab-wedge coupling begins is poorly constrained, but shallow coupling depths < 70 km result in high-temperature mantle flow beneath the forearc, and therefore can be ruled out by the observed low heat flow in forearcs. In forced convection models, the subducting slab drags the base of the mantle wedge downward. In models with strong temperature-dependent viscosity, the down-dragged wedge material is replaced by hot mantle and calculated interface temperatures are several hundred degrees warmer than constant viscosity models [*Kiefer et al.,* 2001].

More realistic models of the mantle wedge flow require dynamical calculations incorporating buoyancy forces (free convection) [e.g., *Davies and Stevenson,* 1992; *Kincaid and Sacks,* 1997]. Local buoyancy forces generated by partial melting can modify the slab-induced flow field in the mantle wedge [Davies and Stevenson, 1992]. If the viscosity of the mantle wedge is low (<6 x 10^{18} Pa s), then the buoyancy generated by partial melting could lead to appreciable upward flow or flow reversal [*Davies and Stevenson,* 1992]. Calculations by *Iwamori* [1997], using a mantle viscosity of 10^{21} Pa s, generated thermal buoyancy driven flow approximately $^1/_3$ as vigorous as mechanically driven flow. This result depends strongly on the mantle viscosity structure; temperature-dependent mantle viscosities will result in more vigorous flow that should elevate temperatures in the core of the mantle wedge. *Kincaid and Sack's* [1997] dynamical models showed that the material in the mantle-wedge corner cools and stagnates with time, which is consistent with the low surface heat flow observed in forearcs.

Similar slab-mantle interface temperatures are predicted by thermal models incorporating forced convection (viscous traction) and combined forced and free convection (viscous traction and thermal buoyancy) (Figure 2). In all models a cool boundary layer forms along the base of the mantle wedge and heat must be conducted across this layer in order to reach the slab. For a wide range of subduction parameters, calculated slab-mantle interface temperatures are less than 0.5 ($T_s + T_i$) (Figure 2). However, numerical modeling efforts have yet to explore the possibility of rapid mantle-wedge convection where wedge velocities exceed slab velocities.

Rapid mantle-wedge convection could occur if mantle viscosities are lower than previously considered and a growing body of evidence suggests this may be the case. Laboratory measurements indicate that olivine is dramatically weaker in the presence of water [*Karato and Wu,* 1993]; such conditions would likely exist in the mantle wedge above the dehydrating slab. In the northern Cascadia subduction zone, post-seismic uplift data are consistent with viscoelastic deformation models with a mantle-wedge viscosity of 10^{18} to 10^{19} Pa s [*Wang et al.,* 1994] and post-glacial rebound data indicate a mantle wedge viscosity of 5 x 10^{18} to 5 x 10^{19} Pa s [*James et al.,* 2000]. Dynamical models of the Tonga-Kermadec subduction zone by *Billen and Gurnis* [in press] require a low viscosity mantle wedge (a factor of 10 less viscous than the surrounding asthenosphere) in order to decouple the slab from the overriding plate and provide a better match to topographic, gravity, and geoid observations.

The complex rheological structure of the mantle wedge remains a formidable challenge to determining the geometry and vigor of mantle-wedge flow. The viscosity of mantle-wedge peridotite can vary over many orders of magnitude due to variations in temperature (T), pressure (P), strain rate, bulk composition, the amount of hydration, and the local presence of aqueous fluids and silicate melts. Relatively weak rock types (metasediments, metamorphosed oceanic crust, serpentinite) present along the slab-mantle interface will likely control the degree of viscous coupling between the subducting slab and overlying mantle wedge [*Yuen et al.,* 1978]. Current modeling efforts by several different groups are systematically examining these complexities, but the key to constraining the geometry and vigor of mantle-wedge flow may well lie in the seismological and arc geochemical observations.

METAMORPHIC EVOLUTION OF SUBDUCTING SLABS

During subduction, sediments, oceanic crust, and oceanic mantle undergo metamorphic transformations that increase the density of the subducting slab. Many of these metamorphic reactions involve the breakdown of hydrous minerals and release substantial amounts of H_2O [e.g., *Poli and Schmidt,* 1995; *Schmidt and Poli,* 1998]. Most of the H_2O liberated from subducting slabs at depths greater than 10 km is derived from variably hydrated basalts and gabbros in the

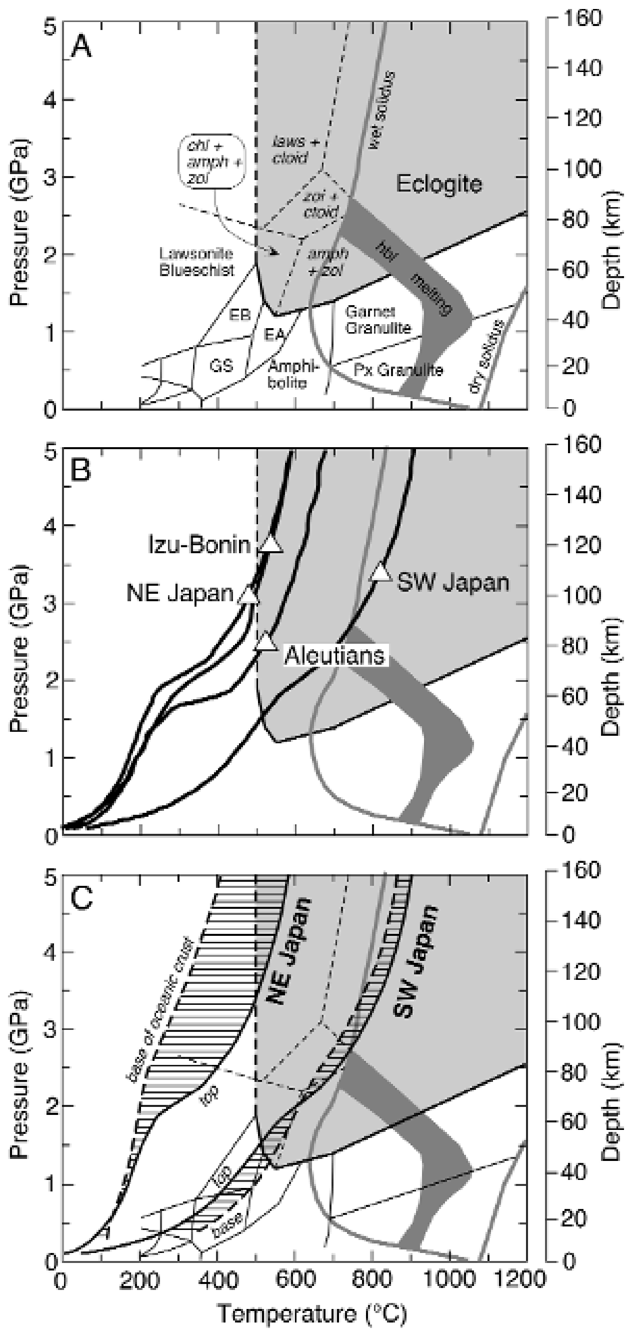

subducting oceanic crust [e.g., *Peacock,* 1990a]. Globally, 1 to 2 x 10^{12} kg of bound H_2O is subducted each year with hydrous minerals in the altered oceanic crust accounting for ~90-95% of this flux [*Ito et al.,* 1983; *Peacock,* 1990a; *Bebout,* 1996].

The volume and composition of pelagic and terrigenous sediments subducted in different subduction zones varies considerably due to variable input, offscraping, and underplating [e.g., *von Huene and Scholl,* 1991]. At shallow depths (<10 km), large amounts of pore waters are expelled by sediment compaction [*Moore and Vrolijk,* 1992]. Structurally bound H_2O is released from sediments during the transformation of opal to quartz (~80 °C), the dehydration of clay mineral to form mica (100-180 °C), and chlorite breakdown (400-600 °C) [*Moore and Vrolijk,* 1992]. In warm subduction zones, mica will dehydrate and/or partially melt at T ~ 800 °C.

H_2O subducted as part of the oceanic crust dominates the H_2O flux into subduction zones. Drill holes and hydrogeologic data show that the uppermost kilometer of the oceanic crust has high porosities of ~10% [e.g., *Becker et al.,* 1989; *Fisher,* 1998]. Collapse of this porosity at temperatures of perhaps 300-500 °C will expel substantial amounts of pore water. Alternatively, interstitial pore water may react to form low-temperature minerals such as zeolites that subsequently dehydrate as the crust subducts. The most important reactions in subducting oceanic crust involve the transformation to eclogite, a relatively dense, anhydrous rock consisting primarily of garnet and omphacite (Na-Ca clinopyroxene) (Figure 3). In a given subduction zone, the depth and nature of eclogite formation and slab dehydration reactions depends on the *P-T* conditions encountered by the subducting oceanic crust. In the relatively warm Nankai subduction zone, subducted oceanic crust passes through the greenschist facies and the transformation to eclogite may occur at ~50 km depth. Calculated *P-T* paths for Nankai intersect mafic partial melting reactions at ~100 km depth and the uppermost oceanic crust may possibly melt (see discussion of adakites below). In contrast, calculated *P-T* paths for relatively cool subduction zones like NE Japan pass through the blueschist facies and eclogite may not form until depths > 100 km (Figure 3C, 4).

Figure 3. Calculated pressure-temperature (*P-T*) paths and metamorphic conditions encountered by subducting oceanic crust. (A) *P-T* diagram constructed for metabasaltic compositions showing metamorphic facies (solid lines), hydrous minerals stable in the eclogite facies (italics), and partial melting reactions (dark gray lines) [see references in *Peacock et al.,* 1994; *Poli and Schmidt,* 1995; *Peacock and Wang,* 1999]. EA, epidote-amphibolite facies; EB, epidote-blueschist facies; GS, greenschist facies; Px Granulite, pyroxene granulite facies; amph, amphibole, chl, chlorite, ctoid, chlorotoid, laws, lawsonite; hbl, hornblende; zoi, zoisite. (B) Calculated *P-T* paths for top of the subducting oceanic crust in four subduction zones. Triangles represent *P-T* conditions directly below the volcanic front. (C) Calculated *P-T* conditions for top and base of oceanic crust subducted beneath NE and SW Japan [after *Peacock and Wang,* 1999].

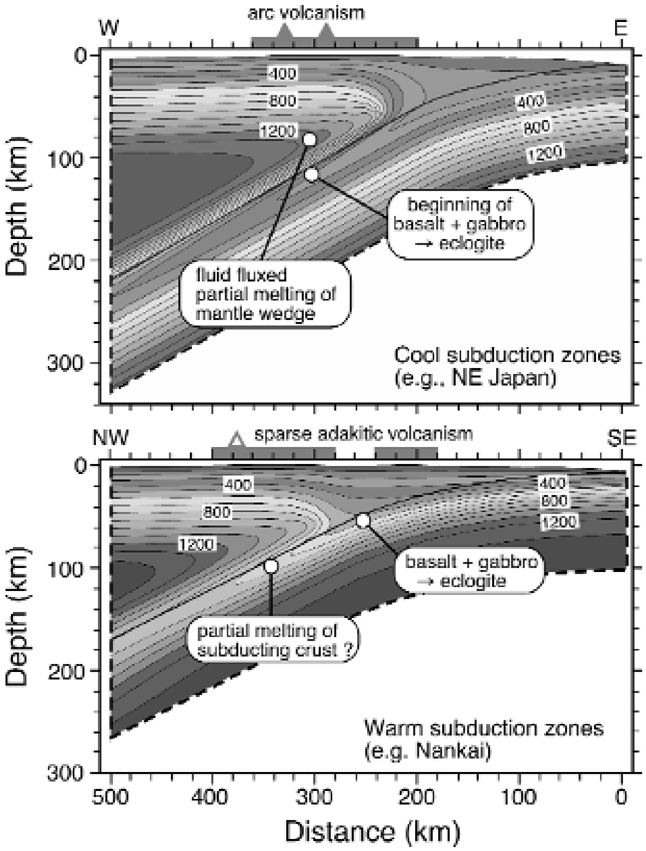

Figure 4. Location of important petrologic processes in (A) cool and (B) warm subduction zones.

In cool subducting slabs, hydrous minerals stable in the blueschist and low-temperature eclogite facies are capable of transporting H_2O to depths > 200 km. Recent experiments do not support earlier models linking the volcanic front to specific dehydration reactions in the subducting slab. On the contrary, the progressive metamorphism of metabasalts involves complex, continuous reactions that occur over a range in *P-T* space [e.g., *Spear,* 1993; *Schmidt and Poli,* 1998] and temperature-dependent dehydration reactions will be smeared out over a considerable depth range. Experiments conducted on metabasaltic compositions demonstrate that important hosts for H_2O in subducting oceanic crust include amphibole, lawsonite, phengite (mica), chlorite, talc, chlorotoid, and zoisite [e.g., *Pawley and Holloway,* 1993; *Poli and Schmidt,* 1995]. Amphibole (2 wt % H_2O) and lawsonite (11 wt % H_2O) are particularly important hosts for H_2O in subducting mafic rocks. In cool subducting slabs, amphibole dehydrates at ~75 km depth whereas lawsonite remains stable to depths > 200 km [*Pawley and Holloway,* 1993; *Poli and Schmidt,* 1995].

The extent to which the subducting oceanic mantle is hydrated is not known. At moderate to fast spreading ridges, hydrothermal circulation appears largely restricted to crustal levels; in contrast, at slow-spreading ridges, ultramafic rocks are tectonically emplaced at shallow depths and serpentinization is common [e.g., *Buck et al.,* 1998]. In addition to hydrothermal circulation at mid-ocean ridges, seawater may infiltrate the oceanic mantle along fracture zones and in the trench—outer rise region causing serpentinization. Large outer-rise earthquakes commonly rupture the oceanic mantle [e.g., *Christensen and Ruff,* 1988] and these highly permeable faults may promote hydrothermal circulation and alteration of the oceanic mantle [*Peacock,* 2001]. Because serpentine minerals contain ~13 wt % H_2O, even small amounts of serpentinization can contribute significantly to the total amount of H_2O entering a subduction zone.

If the subducting mantle contains serpentine and/or other hydrous minerals, then dehydration reactions will release H_2O from the mantle part of the subducting slab. Antigorite serpentine breaks down to form olivine + orthopyroxene + H_2O at 600-700 °C at pressures between 2 and 5 GPa [*Ulmer and Trommsdorff,* 1995; *Wunder and Schreyer,* 1997]. At higher pressures antigorite breaks down to form olivine + hydrous phase A + H_2O [*Wunder and Schreyer,* 1997; *Bose and Navrotsky,* 1998]. In warm subducting slabs, we would expect serpentine dehydration to be essentially complete by 100 km depth with only minor amounts of H_2O possibly subducted to greater depth by amphibole or chlorite. In cool subducting slabs, serpentine dehydration will not occur until 150-250 km depth and stable hydrous minerals such as phase-A may transport H_2O to even greater depths.

At depths of 400 to 670 km, olivine in the subducting mantle transforms to denser polymorphs (wadsleyite, ringwoodite) and then to perovskite + magnesiowustite at 660 km depth [e.g., *Kirby et al.,* 1996a]. These solid-solid reactions increase the density of the subducting slab. A number of studies [e.g., *Green and Burnley,* 1989; *Kirby et al.,* 1991; 1996a] suggest that deep-focus earthquakes (>300 km depth) may be caused by transformational faulting asso-ciated with the metastable reaction of olivine to denser polymorphs.

What happens to the H_2O liberated from the subducting slab? We expect H_2O to migrate upward and updip, primarily by channelized (focused) flow along faults and high permeability horizons [*Peacock,* 1990a; *Bebout,* 1991]. Most water may ultimately reach the seafloor or land surface. The widespread occurrence of low salinity fluids emanating from accretionary prisms provides direct evidence for deep dehydration fluids reaching the seafloor [*Moore and Vrolijk,* 1992]. The H_2O generated by compaction and low-temperature reactions should elevate fluid pressures and promote faulting along the subduction thrust. As discussed below, H_2O released at depths > 40 km may trigger intraslab earthquakes through dehydration embrittlement [*Kirby et al.,* 1996b].

A portion of the water released from the subducting slab infiltrates the overlying mantle wedge forming hydrous minerals, such as serpentine, brucite, and talc. Hydration will dramatically alter the rheological properties of the wedge, particularly along the slab-mantle interface. In the Mariana forearc, active serpentine mud volcanoes provide dramatic evidence for hydration of the mantle wedge [*Fryer et al.,* 1999]. Serpentine and other hydrous minerals in the forearc mantle may control the downdip limit of subduction thrust earthquakes [*Hyndman et al.,* 1997; *Peacock and Hyndman,* 1999]. At depths >100 km, water released from the subducting slab can trigger partial melting in the overlying mantle wedge.

Paleosubduction zones contain blueschists and low-temperature eclogites that provide insight into the thermal and petrologic structure of subducting slabs. Rigorously inverted metamorphic *P-T* data is difficult because, in general, we do not know the convergence rate at the time these rocks were subducted. Blueschist-facies metabasaltic clasts recovered from an active serpentine mud volcano in the Mariana forearc record T = 150-250 °C at P = 0.5-0.6 GPa [*Maekawa et al.,* 1993] and suggest shear stresses of ~20 MPa along the subduction thrust [*Peacock,* 1996]. Blueschist-facies metasedimentary rocks record subsolidus conditions along the slab interface and are consistent with thermal models with modest to no shear heating [*Peacock,* 1992].

Not all paleosubduction zones record high *P/T* conditions. For example, amphibolite-facies rocks in the Santa Catalina schist complex (southern California) record peak metamorphic conditions of T = 640-750 °C at P = 0.8-1.1 GPa [*Sorensen and Barton,* 1987]. Thermal models predict that slab interface temperatures are relatively high during the initial stages of subduction and decrease over time [*Peacock,* 1990a; *Peacock et al.,* 1994]. Such cooling is well recorded by the successive underplating of greenschist-facies (~500-600 °C) and blueschist-facies (~300-400 °C) units on Santa Catalina Island [*Platt,* 1975; *Bebout,* 1991; *Grove and Bebout,* 1995]. Similarly, eclogite blocks (T ~ 500 °C, P ~ 1-1.5 GPa) in the Franciscan Complex yield the oldest radiometric ages and formed during the early stages of subduction [*Cloos,* 1985].

ARC VOLCANISM

Arc lavas provide important information about subduction zones and petrological and geochemical data may be inverted to gain insight into the thermal and petrologic structure at depth. Basalts are common in many arcs which strongly suggests partial melting of the ultramafic mantle wedge as opposed to the mafic oceanic crust. Glass inclusions in mafic arc lavas exhibit a wide range in H_2O contents from 0.2 to 6 wt % H_2O [e.g., *Sisson and Grove,* 1993; *Roggensack et al.,* 1997; *Newman et al.,* 2000]. Relatively wet magmas reflect the importance of H_2O flux melting in the mantle wedge [e.g., *Gill,* 1981] whereas relatively dry arc magmas may result from adiabatic decompression of the mantle [e.g., *Sisson and Bronto,* 1998]. In the Cascades volcanic arc, dry basaltic magmas last equilibrated with the mantle at T = 1300-1450 °C and P = 1.2-2.2 GPa corresponding to depths of 36-66 km [*Elkins Tanton et al.,* 2001]. Similar mantle-magma equilibration conditions have been inferred by *Tatsumi et al.* [1983] and *Sisson and Bronto* [1998]. Mantle-wedge temperatures in the models depicted in Plate 1 exceed 1300 °C, but at substantially greater depth (>80 km) and generally behind the volcanic front. Most likely this discrepancy results from the simple constant-viscosity wedge-flow model; models employing a temperature-dependent viscosity [e.g., *Furukawa, 1993; Kiefer et al.,* 2001] yield higher mantle-wedge temperatures at shallower depths. In addition, mantle-magma equilibration temperatures may record locally hot mantle conditions beneath arc volcanoes and may not reflect mantle wedge temperatures beneath the entire arc.

Specific minor and trace elements of arc lavas (e.g., K, other large-ion lithophile elements, B, Be, Th, and Pb) appear to be derived from the subducting slab [e.g., *Gill,* 1981; *Hawkesworth et al.,* 1993; *Plank and Langmuir,* 1993; *Davidson,* 1996; *Elliot et al.,* 1997]. Geochemical studies of high-pressure metamorphic rocks have shown that white mica (specifically, a Si-rich muscovite called phengite) is the dominant host for many of these "slab" elements [*Domanik et al.,* 1993]. Most of these slab elements are readily transported in aqueous fluids, but recent experimental mineral-fluid partitioning data suggest that the efficient transport of Be and Th from slab sediments into arc magmas may require sediment melting [*Johnson and Plank,* 1999].

Melting of pelagic sediment at 2-4 GPa requires T > 650-800 °C [*Nichols et al.,* 1996; *Johnson and Plank,* 1999]. Thermal models suggest that such high temperatures are achieved along the slab interface only in unusually warm subduction zones, such as Nankai and Cascadia, where young, hot lithosphere enters the trench. Thermal models of most subduction zones suggest slab interface temperatures are 150-300 °C cooler than required for sediment melting. There are several possible ways to reconcile the high temperatures required for sediment melting with the lower temperatures predicted by thermal models. Rapid convection in the mantle wedge might lead to higher slab temperatures than predicted by existing models in which wedge flow velocities are less than slab velocities. Subducted sediments may melt, but not at the slab interface; for example, sediments might be emplaced into the warmer overlying wedge by diapirism or tectonic intrusion. Alternatively, aqueous fluids may effectively transfer Th and Be into the mantle wedge if fluid fluxes are sufficiently high or if the fluid contains different complexing anions than the experiments. Finally, Th and Be mineral-fluid partition coefficients may be substantially lower (i.e., more strongly partitioned into the fluid) at 500 °C than at 700 °C (the experimental conditions) because the stable mineralogy is different.

Adakites are relatively rare high-Mg andesites with distinctive geochemical characteristics (e.g., light REE enrichment, heavy REE depletion, high Sr) that suggest they formed from partial melts of subducted, eclogite-facies oceanic crust [*Kay,* 1978; *Defant and Drummond,* 1990]. Thermal models predict that partial melting of oceanic crust should only occur where very young oceanic lithosphere is subducted [*Peacock et al.,* 1994]. Recent adakitic lavas present in southern Chile, southwest Japan (Daisen and Sambe volcanoes), Cascadia (Mt. St. Helens), and Panama are underlain by unusually warm subducting crust [e.g., *Peacock et al.,* 1994; Plate 1C]. The type locality for adakite, Adak Island in the Aleutians, represents a striking exception to the general correlation between adakites and warm subducting oceanic crust [*Kay,* 1978; *Yogodzinski and Kelemen,* 1998]. Because the convergence rate and plate age are similar, the thermal structure of the Aleutian arc at Adak Island should be similar to cool thermal structure at Umnak Island, located 600 km to the east (Plate 1D). I do not have a good explanation for the Adak Island adakite locality – perhaps there is another eclogite source, such as a remnant slab, in the Adak mantle wedge? If adakites were common in volcanic arcs, then one might argue that the thermal models are in serious error, but adakites are relatively rare and, in general, occur where young, warm lithosphere is being subducted.

SEISMOLOGICAL OBSERVATIONS

In global and regional seismic tomographic studies, subducting slabs are readily imaged as high velocity, low attenuation regions which reflect the overall cool nature of the slab [e.g., *Zhao et al.,* 1994]. More detailed seismological investigations, using converted phases and waveform dispersion, reveal a thin (<10 km thick), dipping low-velocity layer coinciding with the zone of thrust and intermediate-depth earthquakes [e.g., *Hasegawa et al.,* 1994; *Helffrich,* 1996; *Abers,* 2000]. Thin dipping low-velocity layers have been observed in the Alaska, central Aleutian, Cascadia, northern Kurile, NE Japan, and Nankai subduction zones [e.g., *Fukao et al.,* 1983; *Matsuzawa et al.,* 1986; *Cassidy and Ellis,* 1993; *Abers and Sarker,* 1996; *Helffrich,* 1996; *Abers,* 2000]. In contrast, a high-velocity layer is observed in the Tonga-Kermadec subduction zone [*Ansell and Gubbins,* 1986]. The seismic velocity of eclogite is comparable to mantle peridotite, thus the dipping low seismic-velocity layer is generally interpreted as subducted oceanic crust that has not transformed to eclogite. The low-velocity layer extends to 60 km depth beneath SW Japan [*Fukao et al.,* 1983] and to 150 km depth beneath NE Japan [*Hasegawa et al.,* 1994], in good agreement with the predicted depth of eclogite transformation (Figure 3C) [*Peacock and Wang,* 1999]. Alternatively, the deeper extent of the low-velocity layer in the cooler NE Japan subduction zone may reflect the sluggish kinetics of the anhydrous gabbro to eclogite reaction [*Kirby et al.,* 1996b].

Subduction zones are regions of intense earthquake activity reflecting complex stresses generated by the interaction between the forces that drive and resist subduction, slab deformation (bending, unbending, flexure), thermal expansion, and metamorphic densification reactions [e.g., *Isacks and Barazangi,* 1977; *Spence,* 1987]. At depths > 40 km, high pressure and temperature should inhibit brittle behavior, but earthquakes in subduction zones occur as deep as 670 km. *Kirby et al.* [1996b] proposed that intermediate-depth earthquakes (50-300 km depth) are triggered by dehydration embrittlement associated with the transformation of metabasalt and metagabbro to eclogite within subducting oceanic crust. *Davies* [1999] proposed a related hypothesis linking intermediate-depth earthquakes to hydrofracturing of the subducting oceanic crust. Earthquakes that define the lower plane of double seismic zones, observed in a number of cool subducting slabs, may be triggered by serpentine dehydration reactions [*Peacock,* 2001].

The depth extent of intraslab earthquakes in NE and SW Japan agrees well with the predicted depth of dehydration reactions in the subducting oceanic crust [*Peacock and Wang,* 1999; *Hacker et al.,* 2000]. Beneath NE Japan, intraslab earthquake activity peaks at 125 km depth and extends to >200 km depth [*Hasegawa et al.,* 1994; *Kirby et al.,* 1996b]. Calculated *P-T* paths for NE Japan predict garnet-forming dehydration reactions will begin in the subducted oceanic crust at ~110 km depth and hydrous minerals remain stable to >160 km depth (Figure 3C). Beneath Shikoku (SW Japan), intraslab seismicity ceases at 50-65 km depth [*Nakamura et al.,* 1997]. Calculated *P-T* paths for SW Japan suggest major dehydration of the subducted oceanic crust should occur at ~50 km depth associated with the formation of eclogite; hydrous minerals may persist to 90 km depth (Figure 3C). The lack of intraslab earthquakes at depths > 65 km beneath SW Japan may reflect the onset of ductile slab behavior at $T > 600$ °C [*Peacock and Wang,* 1999] or the relatively small amount of dehydration expected after eclogite formation.

RECENT ADVANCES

Significant progress has been made on many fronts since the Subduction Factory Theoretical and Experimental Institute meeting in Eugene, Oregon, in August, 2000. In this section, I highlight recent advances in the thermal modeling of subduction zones and the connection between intermediate-depth earthquakes and metamorphic dehydration reactions in the subducting slab.

New numerical models have explored the effect of mantle-wedge rheology on the thermal and melting structure of subduction zones. *Van Keken et al.* [2002] constructed a new set of finite element models with high spatial resolution (400 m) and temperature- and stress-dependent olivine rheology for the mantle wedge. Compared to *Peacock and Wang's* [1999] isoviscous model (Plate 1A), *van Keken et al.'s* [2002] models predict higher temperatures within the mantle wedge and along the subduction interface (Figures 5 and 6). Predicted slab interface temperatures beneath the NE Japan volcanic front of 475 °C for the isoviscous case [*Peacock and Wang,* 1999] increase to 610 °C with higher spatial resolution and to 810 °C with more realistic olivine rheology [*van Keken et al.,* 2002] (Figure 6). The higher predicted temperatures suggests that partial melting may occur along the slab interface. Similarly, *Kelemen et al.* [this volume] found that using a T-dependent viscosity for the mantle wedge leads to possible melting of subducted crust over a wider range of convergence rates and plate ages than previously suggested (e.g., subduction of 50 Ma lithosphere at 60 mm/yr). Predicted temperatures within the subducting slab are less affected by the assumed mantle-wedge rheology and slab P-T paths remain subsolidus (Figure 6). *Van Keken et al.* [2002] suggest that the high thermal gradients perpendicular to slab interface could explain the conflicting geochemical evidence for sediment melting and basalt dehydration.

Compared to isoviscous mantle-wedge models, models with a T-dependent mantle-wedge viscosity yield substantial decompression melting in the wedge and high temperatures at shallow depth beneath the arc that are in better agreement with petrological observations [*Kelemen et al.,* this volume; *van Keken et al.,* 2002; *Conder et al.,* 2002]. In isoviscous mantle-wedge models, the 1300 °C wedge isotherm is not reached until 80-90 km depth (e.g., Plate 1). In T-dependent mantle-wedge viscosity models, the 1300 °C isotherm is reached at shallower depths of 45 to 60 km beneath the arc [*Conder et al.,* 2002; *Kelemen et al.,* this volume; van *Keken et al.,* 2002]. In *Conder et al.'s* [2002] model, flow induced by the subducting slab erodes the lower part of the overriding plate leading to enhanced decompression melting and flow into the corner of the mantle wedge. Similar thinning of the upper thermal boundary layer occurs in the models presented by *Kelemen et al*. [this volume] and *van Keken et al*. [2002].

Significant differences among the thermal models remain, most notably with respect to the viscous coupling along the

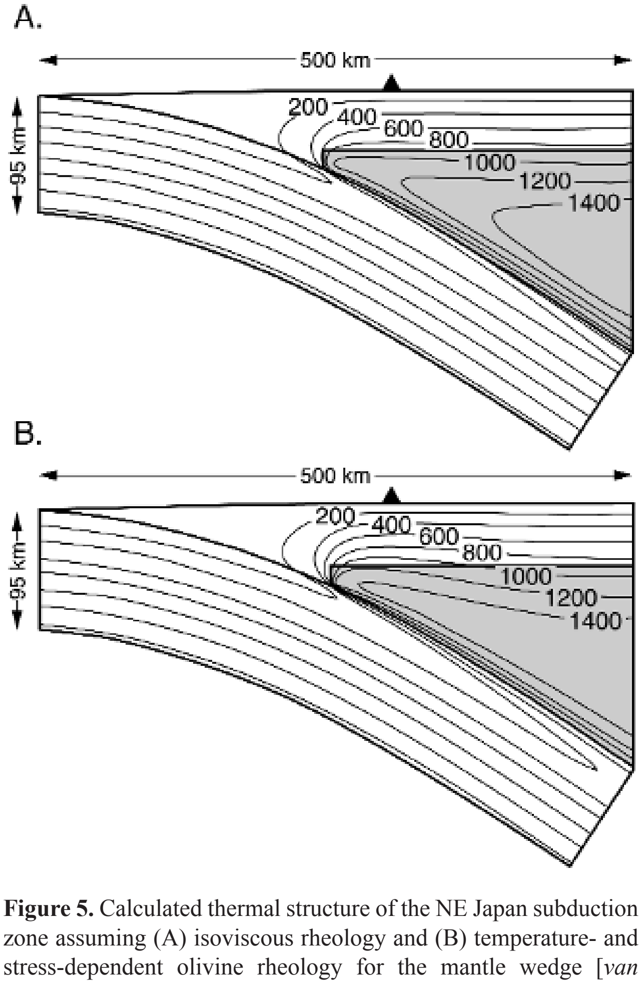

Figure 5. Calculated thermal structure of the NE Japan subduction zone assuming (A) isoviscous rheology and (B) temperature- and stress-dependent olivine rheology for the mantle wedge [*van Keken et al.,* 2002]. Models use the same geometry, heat sources, and boundary conditions as isoviscous model for NE Japan presented by *Peacock and Wang* [1999]. Gray shading = mantle wedge, black triangle = volcanic front. Contour interval = 200 °C.

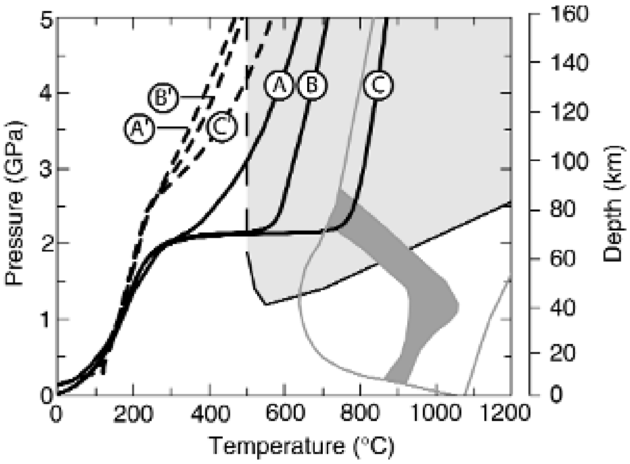

Figure 6. Calculated pressure-temperature conditions for top (solid lines) and base (dashed lines) of oceanic crust subducted beneath NE Japan for three different finite element models. A, A' = isoviscous mantle wedge with spatial resolution on the order of 5 km [*Peacock and Wang,* 1999]. B, B' = isoviscous mantle wedge with 400 m spatial resolution [*van Keken et al.,* 2002]. C, C' = temperature- and stress-dependent mantle wedge rheology with 400 m spatial resolution [*van Keken et al.,* 2002]. See Figure 3A for key to phase diagram.

slab-wedge interface. As demonstrated by *Furukawa* [1993], the depth at which the slab becomes viscously coupled to the mantle wedge strongly influences the thermal structure of the mantle wedge and the degree of decompression melting. As discussed above, the mechanical nature of the slab-wedge interface likely depends on many variables including temperature and the presence of weak materials along the slab-mantle interface. Recent seismological studies indicate that the mantle wedge beneath the forearc is partially serpentinized [*Kamiya and Kobayashi,* 2000; *Bostock et al.,* 2002]. The weak rheology and positive buoyancy of serpentinite will act to isolate the hydrated forearc wedge from the mantle-wedge convection system [*Bostock et al.,* 2002], which is consistent with the low surface heat flow observed in forearcs.

In most thermal models of subduction zones, the velocity field of the subducting plate is defined kinematically [e.g., *Peacock,* 1990; *Davies and Stevenson,* 1992]. *King* [2001] reviewed evidence indicating slabs deform (thicken) significantly as they descend through the upper mantle. Compared to kinematic models, dynamical models that permit slab thickening should yield cooler slab interiors because heat must be conducted a greater distance into the slab interior from the upper and lower slab surfaces [*King,* 2001].

Several groups, using very different approaches, have constructed phase diagrams for metamorphosed basalts in order to gain insight into the dehydration of subducted oceanic crust. Phase diagrams of metabasalts have been constructed based on experimental studies [*Poli and Schmidt,* 1995; *Schmidt and Poli,* 1998], thermodynamic data and a free energy minimization strategy [*Kerrick and Connolly*, 2001], and petrological field observations combined with thermodynamic calculations of key reactions [*Hacker et al.,* 2002a]. At low temperatures and high pressure, where experiments are difficult to conduct and natural samples are rare, there are considerable differences among the proposed phase diagrams, particularly with respect to the stability fields of lawsonite, amphibole, and chlorotoid. At 500 °C and 3 GPa, estimates of the H^{2}O content of fully hydrated metabasalt range from 2.6 wt% H_2O [*Kerrick and Connolly,* 2001] to 1.0 wt% H_2O [*Schmidt and Poli,* 1998] to 0.3 wt% H_2O [*Hacker et al.,* 2002a]. An accurate understanding of the extent and location of dehydration reactions in cool subducting crust requires resolving these differences.

Considerable theoretical and observational advances have been made in our understanding of subduction-zone earthquakes and their connection to metamorphic dehydration reactions in the subducting plate. In an integrated petrological-seismological study of four subduction zones, *Hacker et al*. [2002b] found a strong correlation between intermediate-depth seismicity patterns and the predicted location of dehydration reactions in the subducting oceanic crust and uppermost mantle; this correlation supports *Kirby et al.'s* [1996] dehydration embrittlement hypothesis for intraslab earthquakes. *Seno and Yamanaka's* [1996] proposal that double seismic zones are linked to the dehydration of serpentine in subducting mantle has received additional petrological and seismological support [*Seno et al.,* 2001; Peacock, 2001; *Omori et al.,* 2002]. Based on a statistical analysis of 360 fault plane solutions in the Tonga subduction zone, *Jiao et al.* [2000] demonstrated that earthquakes down to 450 km depth occurred along preexisting asymmetric fault systems that formed prior to subduction. Hydrous minerals present along the preexisting fault zones may explain how these faults zones remain weak to great depth. *Tibi et al.* [2002] found that rupture areas of six large intermediate-depth earthquakes extended 25-50 km parallel to the strike of the slab, but only 4-13 km perpendicular to the slab surface. The orientation of the rupture areas is consistent with the reactivation of trench-parallel faults, with at least the larger earthquakes rupturing the slab mantle. In the SW Japan subduction zone, unusual deep (~30 km) long-period (1-20 Hz) tremors, which persist for several days to weeks, appear to be related to fluids released by slab dehydration reactions [*Obara,* 2002]. Fluids have also been proposed to explain the upward migration of a high *Vp/Vs* region from the hypocenter of the M_W = 8.0 Antofagasta, Chile 1995 thrust earthquake [*Husen and Kissling,* 2001]

CONCLUDING THOUGHTS

The thermal-petrologic models presented in this paper are consistent with a broad range of seismological and arc geochemical observations. For most subduction zones, these models predict that subducting sediments, crust, and mantle will undergo subsolidus metamorphic reactions. Partial melting of subducting materials is predicted to occur only in subduction zones like Nankai where young incoming lithosphere subducts relatively slowly. Tantalizing evidence, such as the Adak Island adakite and mineral-fluid partitioning data on Be and Th, suggests that calculated temperatures along the slab-mantle interface may be too low, at least locally. The incorporation of temperature-dependent viscosity models for the mantle wedge increase calculated slab-mantle interface temperatures, but this is just one of a number of steps we need to take in order to accurately simulate flow in the mantle wedge.

There are a number of important subduction-zone processes that are poorly understood at present and limit our understanding of subduction zones. In my opinion, some of the most important questions to be investigated are (1) the vigor and geometry of mantle-wedge flow induced by the subducting slab and upper-plate extension; (2) variations in thermal parameters and rheology as a function of *P, T,* and composition; (3) metabasaltic phase equilibria and reaction kinetics at low temperatures and high pressure (*e.g.,* 500 °C and 3 GPa); and (4) the amount and distribution of H_2O in the oceanic crust and mantle prior to subduction.

Acknowledgments. I thank the organizers of the NSF Margins Subduction Factory Theoretical and Experimental Institute for arranging a very stimulating and productive conference in Eugene, Oregon. I also thank John Eiler and two anonymous reviewers for providing detailed, constructive reviews. This research was supported by NSF grants EAR 97-25406 and 98-09602

REFERENCES

Abers, G. A., Hydrated subducted crust at 100-250 km depth, *Earth Planet. Sci. Lett., 176,* 323-330, 2000.

Abers, G. A., and G. Sarker, Dispersion of regional body waves at 100- to 150-km depth beneath Alaska: In situ constraints on metamorphism of subducted crust, *Geophys. Res. Lett., 23,* 1171-1174, 1996.

Ansell, J. H., and D. Gubbins, Anomalous high-frequency wave propagation from the Tonga-Kermadec seismic zone to New Zealand, *Geophys. J. R. Astro. Soc., 85,* 93-106, 1986.

Batchelor, G. K., *An introduction to fluid dynamics,* 615 pp., Cambridge University Press, Cambridge, 1967.

Bebout, G. E., Geometry and mechanisms of fluid flow at 15 to 45 kilometer depths in an early Cretaceous accretionary complex, *Geophys. Res. Lett., 18,* 923-926, 1991

Bebout, G. E., Volatile transfer and recycling at convergent margins: Mass balance and insights from high-P/T metamorphic rocks, in *Subduction: Top to Bottom,* edited by Bebout, G. E., *et al.,* 179-193, AGU Geophysical Monograph *96,* Washington, D.C., 1996.

Becker, K., and 24 others, Drilling deep into young oceanic crust, hole 514B, Costa Rica rift, *Rev. Geophys., 27,* 79-102, 1989.

Billen, M. I., and M. Gurnis, A low viscosity wedge in subduction zones, *Earth Planet. Sci. Lett.,* in press, 2001.

Bose, K., and A. Navrotsky, Thermochemistry and phase equilibria of hydrous phases in the system $MgO-SiO_2-H_2O$: Implications for volatile transport to the mantle, J. *Geophys. Res., 103,* 9713-9719, 1998.

Bostock, M.G., R.D. Hyndman, S. Rondenay, and S.M. Peacock, An inverted continental Moho and serpentinization of the forearc mantle, Nature, 417, 536-538, 2002.

Buck, W. R., P. T. Delaney, J. A. Karson, and Y. Lagabrielle (eds.), *Faulting and Magmatism at Mid-Ocean Ridges,* AGU Geophysical Monograph 106, Washington, D.C., 1998.

Carswell, D. A. (ed.), *Eclogite Facies Rocks,* 396 pp., Blackie, London, 1990.

Cassidy, J. F., and R. M. Ellis, S wave velocity structure of the northern Cascadia subduction zone, *J. Geophys. Res., 98* , 4407-4421, 1993.

Christensen, D. H., and L. J. Ruff, Seismic coupling and outer rise earthquakes, *J. Geophys. Res., 93,* 13,421-13,444, 1988.

Cloos, M., Thermal evolution of convergent plate margins: Thermal modeling and reevaluation of isotopic Ar-ages for blueschists in the Franciscan complex of California, *Tectonics, 4* , 421-433, 1985.

Conder, J.A., D.A. Weins, and J. Morris, On the decompression melting structure at volcanic arcs and back-arc spreading centers, Geophys. Res. Lett., in press, 2002.

Davidson, J. P., Deciphering mantle and crustal signatures in subduction zone magmatism, in *Subduction: Top to Bottom,* edited by Bebout, G. E., et al., 251-262, AGU Geophysical Monograph 96, Washington, D.C., 1996.

Davies, J. H., The role of hydraulic fractures and intermediate-depth earthquakes in generating subduction-zone magmatism, *Nature, 398,* 142-145, 1999.

Davies, J. H. and D. J. Stevenson, Physical model of source region of subduction zone volcanics, *J. Geophys. Res., 97,* 2037-2070, 1992.

Defant, M. J., and M. S. Drummond, Derivation of some modern arc magmas by melting of young subducted lithosphere, *Nature, 347,* 662-665, 1990.

LOW RES

DeMets, C., R. G. Gordon, D. F. Argus, and S. Stein, Effect of recent revisions to the geomagnetic reversal timescale on estimates of current plate motions, *Geophys. Res. Lett., 21*, 2191-2194, 1994.

Domanik, K. J., R. L. Hervig, and S. M. Peacock, Beryllium and boron in subduction zone minerals: an ion microprobe study, *Geochim. Cosmochim. Acta, 57,* 1993.

Elkins Tanton, L. T., T. L. Grove, and J. Donnelly-Nolan, Hot, shallow mantle melting under the Cascades volcanic arc, *Geology, 29,* 631-634, 2001.

Elliott, T., T. Plank, A. Zindler, W. White, and B. Bourdon, Element transport from slab to volcanic front at the Mariana arc, *J. Geophys. Res., 102,* 14991-15019, 1997.

Fisher, A. T., Permeability within the basaltic oceanic crust, *Rev. Geophys., 36,* 143-182, 1998.

Forsyth, D., and S. Uyeda, Relative importance of driving forces of plate motion, Geophys. *J. Roy. Astro. Soc., 43,* 163-200, 1975.

Fryer, P., C. G. Wheat, and M. J. Mottl, Mariana blueschist mud volcanism: Implications for conditions within the subduction zone, *Geology, 27,* 103-106, 1999.

Fukao, Y., S. Hori, and M. Ukawa, A seismological constraint on the depth of basalt-eclogite transition in a subducting oceanic crust, *Nature, 303,* 413-415, 1983.

Furukawa, Y., Depth of the decoupling plate interface and thermal structure under arcs, *J. Geophys. Res., 98,* 20,005-20,013, 1993.

Gill, J., *Orogenic Andesites and Plate Tectonics,* 390 pp., Springer-Verlag, New York, 1981.

Green, H. W. I., and P. C. Burnley, A new self-organizing mechanism for deep-focus earthquakes, *Nature, 341,* 733-737, 1989.

Grove, M., and G. E. Bebout, Cretaceous tectonic evolution of coastal southern California: Insights from the Catalina Schist, *Tectonics, 14,* 1290-1308, 1995.

Hacker, B. R., Eclogite formation and the rheology, buoyancy, seismicity, and H_2O content of oceanic crust, in *Subduction: Top to Bottom,* edited by Bebout, G. E., *et al.,* 337-346, AGU Geophysical Monograph *96,* Washington, D.C., 1996.

Hacker, B. R., G. A. Abers, and S. M. Peacock, Phase transformations and the buoyancy, seismicity, and H_2O contents of subduction zones (abs.), *Eos Trans. AGU, 81,* F1372, 2000.

Hacker, B.R., G.A. Abers, and S.M. Peacock, Subduction Factory 1. Theoretical mineralogy, density, seismic wave speeds, and H_2O content, J. Geophys. Res., in press, 2002a.

Hacker, B.R., S.M. Peacock, G.A. Abers, and S.D. Holloway, Subduction Factory 2. Intermediate-depth earthquakes in subducting slabs are linked to metamorphic dehydration reactions, J. Geophys. Res., in press, 2002b.

Hasegawa, A., S. Horiuchi, and N. Umino, Seismic structure of the northeastern Japan convergent plate margin: A synthesis, *J. Geophys. Res., 99,* 22,295-22,311, 1994.

Hawkesworth, C. J., K. Gallagher, J. M. Hergt, and F. McDermott, Mantle and slab contributions in arc magmas, *Ann. Rev. Earth Planet. Sci., 21,* 175-204, 1993.

Helffrich, G., Subducted lithospheric slab velocity structure: Observations and mineralogical inferences, in *Subduction: Top to Bottom,* edited by Bebout, G. E., *et al.,* 215-222, AGU Geophysical Monograph *96,* Washington, D.C., 1996.

Husen, S., and E. Kissling, Postseismic fluid flow after the large subduction earthquake of Antofagasta, Chile, Geology, 29, 847-850, 2001.

Hyndman, R. D., and K. Wang, The rupture zone of Cascadia great earthquakes from current deformation and the thermal regime, *J. Geophys. Res., 100,* 22,133-22,154, 1995.

Hyndman, R. D., M. Yamano, and D. A. Oleskevich, 1997, The seismogenic zone of subduction thrust faults, *Island Arc, 6,* 244-260, 1997.

Isacks, B. L., and M. Barazangi, Geometry of Benioff zones: Lateral segmentation and downwards bending of the subducted lithosphere, in *Island Arcs, Deep Sea Trenches, and Back Arc Basins,* edited by M. Talwani and W. C. Pitman, 99-114, AGU, Washington, D.C., 1977.

Ito, E., D. M. Harris, and A. T. J. Anderson, Alteration of oceanic crust and geologic cycling of chlorine and water, *Geochim. Cosmochim. Acta, 47,* 1613-1624, 1983.

Iwamori, H., Heat sources and melting in subduction zones, *J. Geophys. Res., 102,* 14,803-14,820, 1997.

James, T. S., J. J. Clague, K. Wang, and I. Hutchinson, Postglacial rebound at the northern Cascadia subduction zone, *Quaternary Sci. Rev., 19,* 1527-1541, 2000.

Jiao, W., P.G. Silver, Y. Fei, and C.T. Prewitt, Do intermediate- and deep-focus earthquakes occur on preexisting weak zones? An examination of the Tonga subduction zone. J. Geophys. Res., 105, 28,125-28,138, 2000.

Johnson, M. C., and T. Plank, Dehydration and melting experiments constrain the fate of subducted sediments, *Geochem. Geophys. Geosyst., 1,* 1999.

Kamiya, S., and Y. Kobayashi, Seismological evidence for the existence of serpentinized wedge mantle, Geophys. Res. Lett., 27, 819-822, 2000.

Karato, S., and P. Wu, Rheology of the upper mantle: A synthesis, *Science, 260,* 771-778, 1993.

Kay, R. W., Aleutian magnesian andesites: melts from subducted pacific ocean crust, *J. Volc. Geotherm. Res., 4,* 117-132, 1978.

Kelemen, P.B., J.L. Rilling, E.M. Parmentier, L. Mehl, and B.R. Hacker, Flow in the mantle wedge beneath subduction-related magmatic arcs, in Eiler, J. (ed.), The Subduction Factory, AGU Geophysical Monograph, in press, 2002.

Kerrick, D.M., and J.A.D. Connolly, Metamorphic devolatilization of subducted oceanic metabasalts: implications for seismicity, arc magmatism and volatile recycling, Earth Planet. Sci. Lett., 189, 19-29, 2001.

Kiefer, B., P. van Keken, and S. M. Peacock, The thermal structure of subduction zones (abs.), *Eos Trans. AGU, 82,* S411, 2001

Kincaid, C., and I. S. Sacks, Thermal and dynamical evolution of the upper mantle in subduction zones, *J. Geophys. Res., 102,* 12,295-12,315, 1997.

King, S.D., Subduction zones: Observations and geodynamic models, Phys. Earth Planet. Interiors, 127, 9-24, 2001.

Kirby, S. H., W. B. Durham, and L. A. Stern, Mantle phase changes and deep-earthquake faulting in subducting lithosphere, *Science, 252,* 216-225, 1991.

Kirby, S. H., S. Stein, E. A. Okal, and D. C. Rubie, Metastable mantle phase transformations and deep earthquakes in subducting oceanic lithosphere, *Rev. Geophys., 34,* 261-306, 1996a.

Kirby, S. H., E. R. Engdahl, and R. Denlinger, Intraslab earthquakes and arc volcanism: dual physical expressions of crustal and uppermost mantle metamorphism in subducting slabs, in *Subduction: Top to Bottom,* edited by Bebout, G. E., *et al.,* 195-214, AGU Geophysical Monograph *96,* Washington, D.C., 1996b.

Maekawa, H., M. Shozui, T. Ishii, P. Fryer, and J. A. Pearce, Blueschist metamorphism in an active subduction zone, *Nature, 364,* 520-523, 1993.

Matsuzawa, T., N. Umino, A. Hasegawa, and A. Takagi, Upper mantle velocity structure estimated from PS - converted wave beneath the north-eastern Japan Arc, *Geophys. J. Roy. Astro. Soc., 86,* 767-787, 1986.

McKenzie, D. P., Speculations on the consequences and causes of plate motions, *Geophys. J. Roy. Astro. Soc., 18,* 1-32, 1969.

Molnar, P., and P. C. England, Temperatures, heat flux, and frictional stress near major thrust faults, *J. Geophys. Res., 95,* 4833-3856, 1990.

Moore, J. C., and P. Vrolijk, Fluids in accretionary prisms, *Rev. Geophys.,* 30, 113-135, 1992.

Nakamura, M., H. Watanabe, T. Konomi, and K. Miura, Characteristic activities of subcrustal earthquakes along the outer zone of southwestern Japan, *Annals Disaster Prevention Res. Inst., Kyoto Univ., 40 B-1,* 1997.

Newman, S., E. Stolper, and R. Stern, H_2O and CO_2 in magmas from the Mariana arc and back arc systems, *Geochem. Geophys. Geosyst., 1,* 2000.

Nichols, G. T., P. J. Wyllie, and C. R. Stern, Experimental melting of pelagic sediment, constraints relevant to subduction, , in Subduction: Top to Bottom, edited by Bebout, G. E., *et al.,* 293-298, AGU Geophysical Monograph *96,* Washington, D.C., 1996.

Obara, K., Nonvolcanic deep tremor associated with subduction in southwest Japan, Science, 296, 1679-1681, 2002.

Omori, S., S. Kamiya, H. Maruyama, and D. Zhao, Morphology of the intraslab seismic zone and devolatilization phase equilibria of the subducting slab peridotite, Bull. Earthq. Res. Inst. Univ. Tokyo, 76, 455-478, 2002.

Oxburgh, E. R., and D. L. Turcotte, Thermal structure of island arcs, *Geol. Soc. Amer. Bull., 81,* 1665-1688, 1970.

Pawley, A. R., and J. R. Holloway, Water sources for subduction zone volcanism: new experimental constraints, *Science, 260,* 664-667, 1993.

Peacock, S. M., Thermal effects of metamorphic fluids in subduction zones, *Geology, 15* , 1057-1060, 1987.

Peacock, S. M., Fluid processes in subduction zones, *Science, 248,* 329-337, 1990a.

Peacock, S. M., Numerical simulation of metamorphic pressure-temperature-time paths and fluid production in subducting slabs, *Tectonics, 9,* 1197-1211, 1990b.

Peacock, S. M., Blueschist-facies metamorphism, shear heating, and P-T-t paths in subduction shear zones, *J. Geophys. Res., 97,* 17,693-17,707, 1992.

Peacock, S. M., Thermal and petrologic structure of subduction zones, in *Subduction: Top to Bottom,* edited by Bebout, G. E., *et al.,* 119-133, AGU Geophysical Monograph *96,* Washington, D.C., 1996.

Peacock, S. M., Are the lower planes of double seismic zones caused by serpentine dehydration in subducting oceanic mantle?, *Geology, 29,* 299-302, 2001.

Peacock, S. M., and R. D. Hyndman, Hydrous minerals in the mantle wedge and the maximum depth of subduction thrust earthquakes, *Geophys. Res. Lett., 26,* 2517-2520, 1999.

Peacock, S. M., T. Rushmer, and A. B. Thompson, Partial melting of subducting oceanic crust, *Earth Planet. Sci. Lett., 121,* 227-244, 1994.

Peacock, S. M., and K. Wang, Seismic consequences of warm versus cool subduction zone metamorphism: Examples from northeast and southwest Japan, *Science, 286,* 937-939, 1999.

Plank, T. A., and C. Langmuir, Tracing trace elements from sediment input to volcanic output at subduction zones, *Nature, 362,* 739-742, 1993.

Platt, J. P., Metamorphic and deformational processes in the Franciscan Complex, California: Some insights from the Catalina Schist terrane, *Geol. Soc. Amer. Bull., 86,* 1337-1347, 1975.

Poli, S., and M. W. Schmidt, H_2O transport and release in subduction zones: Experimental constraints on basaltic and andesitic systems, *J. Geophys. Res., 100,* 22,299-22,314, 1995.

Rabinowicz, M., B. Lago, and C. Froidevaux, Thermal transfer between the continetal asthenosphere and the oceanic subducting lithosphere: Its effect on subcontinental convection, *J. Geophys. Res., 85,* 1839-1853, 1980.

Roggensack, K., R. L. Hervig, S. B. McKnight, and S. N. Williams, Explosive basaltic volcanism from Cerro Negro volcano: Influence of volatiles on eruptive style, *Science, 277,* 1639-1642, 1997.

Rowland, A., and J. H. Davies, Buoyancy rather than rheology controls the thickness of overriding mechanical lithosphere at subduction zones, *Geophys. Res. Lett., 26,* 3037-3040, 1999.

Schmidt, M. W., and S. Poli, Experimentally based water budgets for dehydrating slabs and consequences for arc magma generation, *Earth Planet. Sci. Lett., 163* , 361-379, 1998.

Seno, T., D. Zhao, Y. Kobayashi, and M. Nakamura, Dehydration of serpentinized slab mantle: Seismic evidence from southwest Japan, Earth Planets Space, 53, 861-871, 2001.

Sisson, T. W., and T. L. Grove, Temperatures and H_2O contents of low-MgO high-alumina basalts, *Contrib. Mineral. Petrol., 113,* 167-184, 1993.

Sisson, T. W., and S. Bronto, Evidence for pressure-release melting beneath magmatic arcs from basalt at Galunggung, Indonesia, *Nature, 391,* 883-886, 1998.

Sorensen, S. S., and M. D. Barton, Metasomatism and partial melting in a subduction complex: Catalina Schist, southern California, *Geology, 15,* 115-118, 1987.

Spear, F. S., *Metamorphic Phase Equilibria and Pressure-Temperature-Time Paths,* 799 pp., Mineralogical Society of America, Washington D.C., 1993.

Spence, W., Slab pull and the seismotectonics of subducting lithosphere, *Rev. Geophys., 25,* 55-69, 1987.

Stein, C. A., and S. Stein, A model for the global variation in oceanic depth and heat flow with lithospheric age, *Nature, 359,* 123-129, 1992.

Tatsumi, Y., M. Sakuyama, H. Fukuyama, and I. Kushiro, Generation of arc basalt magmas and thermal structure of the mantle wedge in subduction zones, *J. Geophys. Res., 88,* 5815-5825, 1983.

Tibi, R., G. Bock, and C.H. Estabrook, Seismic body wave constraint on mechanisms of intermediate-depth earthquakes, J. Geophys. Res., 107, 10.1029/2001JB000361, 2002.

Tichelaar, B. W., and L. J. Ruff, Depth of seismic coupling along subduction zones, *J. Geophys. Res., 98,* 2017-2037, 1993.

Toksöz, M. N., J. W. Minear, and B. R. Julian, Temperature field and geophysical effects of a downgoing slab, *J. Geophys. Res., 76,* 1113-1138, 1971.

Turcotte, D. L., and G. Schubert, Frictional heating of the descending lithosphere, *J. Geophys. Res., 78,* 5876-5886, 1973.

Ulmer, P., and V. Trommsdorff, Serpentine stability to mantle depths and subduction-related magmatism, *Science, 268,* 858-861, 1995.

van Keken, P.E., B. Kiefer, and S.M. Peacock, High resolution models of subduction zones: Implications for mineral dehydration reactions and the transport of water into the deep mantle, Geochem., Geophys., Geosys., in press, 2002.

von Huene, R., and D. W. Scholl, Observations at convergent margins concerning sediment subduction, subduction erosion, and the growth of continental crust, *Rev. Geophys., 29,* 279-316, 1991.

von Herzen, R., C. Ruppel, P. Molnar, M. Nettles, S. Nagihara, and G. Ekström, A constraint on the shear stress at the Pacific-Australian plate boundary from heat flow and seismicity at the Kermadec forearc, *J. Geophys. Res., 106,* 6817-6833, 2001.

Wang, K., H. Dragert, and H. J. Melosh, Finite element study of uplift and strain across Vancouver Island, *Can. J. Earth Sci., 31,* 1510-1522, 1994.

Wang, K., T. Mulder, G. C. Rogers, and R. D. Hyndman, Case for low coupling stress on the Cascadia subduction fault, *J. Geophys. Res., 100,* 12,907-12,918, 1995.

Wunder, B., and W. Schreyer, Antigorite: High-pressure stability in the system $MgO-SiO_2-H_2O$ (MSH), *Lithos, 41,* 213-227, 1997.

Yogodzinski, G. M., and P. B. Kelemen, Slab melting in the Aleutians: implications of an ion probe study of clinopyroxene in primitive adakite and basalt, *Earth Planet. Sci. Lett., 158,* 53-65, 1998.

Yuen, D. A., L. Fleitout, G. Schubert, and C. Froidevaux, Shear deformation zones along major transform faults and subducting slabs, *Geophys. J. Roy. Astro. Soc., 54,* 93-119, 1978.

Zhao, D., A. Hasegawa, and H. Kanamori, Deep structure of Japan subduction zone as derived from local, regional, and teleseismic events, *J. Geophys. Res., 99,* 22,313-22,329, 1994.

Zhong, S. J., and M. Gurnis, Controls on trench topography from dynamic-models of subducted slabs, *J. Geophys. Res., 99,* 15,683-15,695, 1994.

S. M. Peacock, Department of Geological Sciences, Arizona State University, Box 871404, Tempe, Arizona, 85287-1404. (e-mail: peacock@asu.edu)